CHAPTER 12

Content-Based Image Retrieval Using Zernike Moments for Binary and Grayscale Images

Muhammad Suzuri Hitam, Suraya Abu Bakar, and Wan Nural Jawahir Wan Yussof

Image features play a vital role in image retrieval. This chapter presents the use of Zernike moment features for retrieving the binary and gray level images from established image databases. To retrieve a set of similar category of images from an image database, up to 25 Zernike moment features from order zero to order 8 were utilized and experimented in this chapter. A total of 1400 binary images from MPEG-7 dataset and 1440 images from a COIL-20 dataset were used to evaluate the capability of Zernike moments features for image retrieval. The experimental results show that Zernike moments implementation is suitable for image retrieval due to rotation invariance and fast computation.

Muhammad Suzuri Hitam, Suraya Abu Bakar, Wan Nural Jawahir Hj Wan Yussof
School of Informatics and Applied Mathematics, University Malaysia Terengganu
21030 Kuala Terengganu, Malaysia
e-mail: suzuri@umt.edu.my, surayag@gmail.com, wannurwy@umt.edu.my

Editor: G.A. Papakostas, *Moments and Moment Invariants - Theory and Applications*

DOI: 10.15579/gcsr.vol1.ch12, GCSR Vol. 1,

12.1 Introduction

Image retrieval is a technique of browsing, searching and retrieving images from a large database of digital images collections. The availability of large amount of digital images collections necessitates powerful algorithms for image retrieval. Thus, in searching for an object from a large collection of digital images, it is necessary to develop appropriate information systems to efficiently manage these collections. Therefore, a number of image searching [24, 14] and image retrieval systems [18, 13, 30] have been proposed. One of the well-known techniques in image retrieval is Content Based Image Retrieval (CBIR). CBIR system extracts image information known as features that are used to retrieve relevant images from image database that best match with query image. Since there are huge potential applications utilizing this technique, CBIR becomes a popular research area in image retrieval [3, 28, 25, 6]. Basically, CBIR extracts appropriate low-level features such as color, texture, shape or their combinations.

Shape plays an important role in describing image contents and for CBIR purpose, a shape representation should be robust, invariant, easy to derive and match. In describing a meaningful shape representation, a common method is to use a moment descriptor. The feature of image moments has been widely used in the area of computer vision and robotics such as object identification techniques [10, 19, 23]. Recently, the famous application of image retrieval using moment based methods include medical image retrieval [15, 2], trademark image retrieval [5, 1] and shape based image retrieval [7, 11]. Moment functions capture global features and thus are suitable for shape recognition. Some moment functions exhibit natural invariance properties including invariance to translation, rotation or scaling. There are various examples of moments including geometric, complex, radial and orthogonal. Geometric moments are widely used in image processing, however these moments are not optimal with respect to information redundancy. Hu [12] was the first to introduce seven moment-based image invariants that set out the mathematical foundation for two-dimensional moment invariants. Hu defined seven moment invariants from geometric moments that are invariants to rotation. In order to make the features invariant to translation and scaling, it needs to substitute the geometric moment with the normalized central moment. These moment values are invariant to translation, rotation and scaling. Unfortunately, the computation of higher order moment invariants, is a quite complicated process. To overcome the shortcomings associated with geometric moments, Teague [26] suggested the use of orthogonal moments.

Orthogonal moments can be categorized into discrete and continuous orthogonal moments. The most well known orthogonal moment families include Zernike [26, 16], Pseudo-Zernike [27], Fourier-Mellin [8, 4], Legendre [22], Tchebichef [21] and Krawtchouk [29] that were applied in most image processing applications. Moments with a continuous orthogonal base set such as Legendre [22], Zernike Moments and Pseudo-Zernike can be used to represent an image with minimum redundancy information. Tchebichef [21], sometimes also written as Chebyshev, and Krawtchouk are among the famous discrete orthogonal moments. The benefits of the orthogonal moments are the unique description of an object with low information redundancy and their ability to perfectly reconstruct an image. Since the continuous orthogonal moments have these properties, this research is focused on continuous orthogonal mo-

ments and a brief description of the benefits is reviewed. Teague [26] introduced the use of Zernike moments in image analysis to recover the image from moment invariants based on the theory of orthogonal polynomials in 1980. Zernike moments are rotation invariant, robust to noise and their accuracy in terms of their discretization errors and reconstruction power has been discussed in [17]. Zernike moments are also able to store the image information with minimal information redundancy and have the property of being rotational invariant. Based on these properties of Zernike Moments, this chapter focuses on experimental evaluation of Zernike moments for image retrieval.

Good features should have the following properties including efficiency, invariance, robustness, distinctiveness, accuracy and many more. In terms of efficiency, the features in an image should be detected fast, in time critical applications. As far as the invariance properties are concerned, it is preferred to detect features that are unaffected by the common mathematical transformations. Typically, the tackled deformations relative to robustness are image noise, blurring and compression. The intensity patterns underlying the detected features should show a lot of variations such that features can be distinguished and matched later on. The detected features also should be accurately localized. This research focuses on the properties including invariance and efficiency in retrieving the similar images.

This chapter implements a Zernike moment method for retrieving similar looking images from image database as in the image query. Experimental evaluation has been carried out to verify the capability of the proposed method by retrieving similar looking binary as well as grayscale images from established image database. The rest of this chapter is organized as follows. Section 12.2 gives a brief review and definitions of Zernike moments. In Section 12.3, the system architecture of Zernike moments implementation is presented. Section 12.4 presents experimental results for both binary and grayscale image databases followed by some related analysis and discussion. The conclusions are presented in the final Section 12.5.

12.2 Zernike Moments

12.2.1 Definitions

The complex Zernike moment of order p with repetition q for an image function $I(\rho, \theta)$ in polar coordinates is defined as in Eq.(12.1).

$$A_{pq} = \frac{p+1}{\pi} \sum_{\rho} \sum_{\theta} \left[V_{pq}(\rho, \theta)\right]^* I(\rho, \theta), \ s.t. \ \rho \leq 1, \tag{12.1}$$

where $V_{pq}(\rho, \theta)$ is a Zernike polynomial that forms a a complete orthogonal set over the interior of the unit disc of $x^2 + y^2 \leq 1$.

12.2.2 Zernike Polynomials

In polar coordinates, the form of the polynomial can be expressed as in Eq.(12.2). The functions $V_{pq}(\rho, \theta)$ denotes Zernike polynomials of order p with repetition q.

Table 12.1: Radial polynomial (R_{pq}) computation.

p \ q	0	1	2	3	4	5	6	7	8	9
0	R_{00}	-								
1	-	R_{11}								
2	R_{20}	-	R_{22}							
3	-	R_{31}	-	R_{33}						
4	R_{40}	-	R_{42}	-	R_{44}					
5	-	R_{51}	-	R_{53}	-	R_{55}				
6	R_{60}	-	R_{62}	-	R_{64}	-	R_{66}			
7	-	R_{71}	-	R_{73}	-	R_{75}	-	R_{77}		
8	R_{80}	-	R_{82}	-	R_{84}	-	R_{86}	-	R_{88}	
9	-	R_{91}	-	R_{93}	-	R_{95}	-	R_{97}	-	R_{99}

$$V_{pq}(\rho,\theta) = R_{pq}(\rho)\, exp(-jq\theta), \tag{12.2}$$

where

$j = \sqrt{-1}$
p: positive integer or zero; i.e. $p = 0, 1, 2, ..., \infty$
p: positive integer subject to constraint $p - |q|$ =even, $q \leq p$
ρ: length of vector from origin to (x, y) pixel, i.e. $\rho = \sqrt{x^2 + y^2}$
θ: angle between the vector ρ and the x axis in the counter clockwise direction

The radial polynomial $R_{pq}(\rho)$ is defined as in Eq.(12.3):

$$R_{pq}(\rho) = \sum_{s=0}^{(p-|q|)/2} \frac{(-1)(p-s)!}{s!\,(p+|q|-s)!\,(p-|q|-s)} \rho^{p-2s}. \tag{12.3}$$

The radial polynomial up to order p will be computed until the meaningful or similar features were obtained. The computation of radial polynomial with order p and repetition q is shown in Table 12.1. Radial polynomial computation up to order 9 was shown in Table 12.1 that is labeled as R_{pq}.

The Zernike polynomials will have to be calculated at each pixel position given that Zernike moments defined in polar coordinates. By using a square-to-circular image transformation as proposed by Mukundan and Ramakrishnan [22], Zernike polynomial only needs to be computed once for all pixels mapped to the same circle. Figure 12.1 shows the schematic of square-to-circular image transformation.

From Fig.(12.1), the image pixels as arranged along concentric squares can be mapped to concentric circles. The image coordinate system (x, y) is defined with the origin at the center of the square pixel grid. The pixel coordinates of the transformed

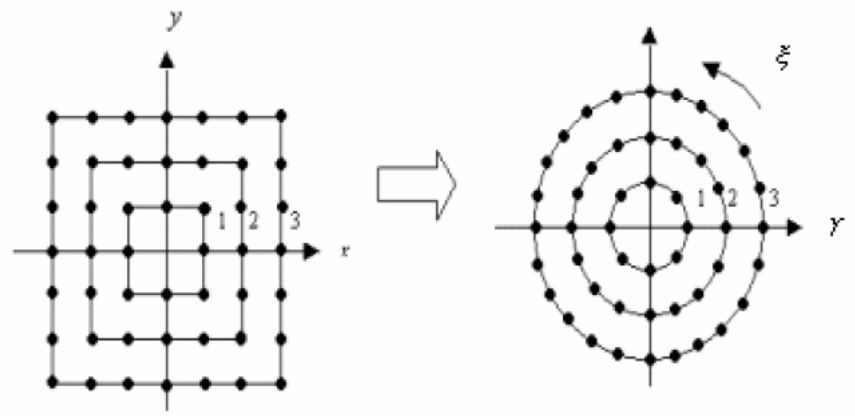

Figure 12.1: Schematic of square-to-circular image transformation.

circular image can be represented by γ and ξ. The values γ and ξ denote the radius of the circle and the position index of the pixel on the circle, respectively. Both γ and ξ values can be obtained as follows:

$$\gamma = \max\{|x|, |y|\}$$

$$if\ |x| = \gamma,\ then\, \xi = 2(\gamma - x)\frac{y}{|y|} + \frac{xy}{\gamma}$$

$$if\ |y| = \gamma,\ then\, \xi = 2y - \frac{xy}{\gamma}$$

It is assumed that the image intensity values are preserved under the transformation, so that $I(x, y) = I(\gamma, \xi)$. Therefore, values of the coordinate indices must be in the ranges as follows:

$$-N/2 \le x, y \le N/2;\ \ 0 \le \gamma \le N/2;\ \ 1 \le \xi \le 8\gamma$$

where N is the image size. Then the polar coordinates p, q of the pixel (γ, ξ) are normalized as in Eq.(12.4):

$$\rho = 2\gamma/N;\ \ \theta = \pi\xi/(4\gamma) \tag{12.4}$$

12.3 System architecture

The architecture of Zernike Moments implementation for image retrieval is shown in Fig.(12.3). There are two main phases in the system. The first phase is an offline phase where Zernike moments' properties were extracted from image database. The features that have been extracted are then stored as feature vector in feature database.

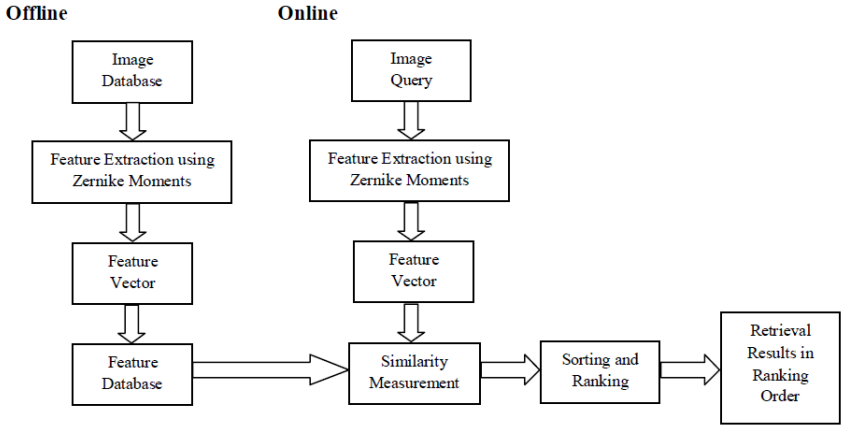

Figure 12.2: System architecture of Zernike moments for image retrieval.

The second phase is an online phase where a user can select any image query from image database. Similarly, a set of Zernike moment features will be extracted from the query image. These features will later be compared with the same features from the set of previously stored features in the features database. Similarity measurement, i.e. Euclidean distance is used to compute the distance measure between the features from the query image and each feature vector of the database images. The distance measure results will be used to sort and rank the images inside the database accordingly, before a set of retrieval output is displayed to the user.

To obtain the similarity between images, let $V^{(k)} = \left\{v_1^{(k)}, v_2^{(k)}, v_3^{(k)} ..., v_n^{(k)}\right\}$ and $Q = \{q_1, q_2, q_3, ..., q_n\}$ denote a feature vector corresponding image k in the database and query image, respectively. The Euclidean distance measures the similarity between query image and each image in the database using the following equation:

$$ED\left(Q, V^{(k)}\right) = \sqrt{\sum_{i=1}^{n}\left(q_i - v_i^{(k)}\right)^2} \tag{12.5}$$

where n is the length of feature vector. The value of k for which the function ED is minimum, is selected as the matched image index.

12.4 Experimental Results and Discussion

In this section, experimental results of Zernike moments' implementation that is carried out by using both binary and grayscale image datasets are presented. The experiments are implemented under the Microsoft Windows XP operating system using MATLAB® version 7.12.0 and on Intel (R) CPU 2.00 GHz with 3.0 GB RAM. The experiments were conducted using the Zernike moments method in testing the capability in retrieving similar look images from the binary MPEG-7 [20] image database and the gray-level COIL-20 [9] image database.

Table 12.2: List of Zernike moments up to order $p = 8$.

p \ q	0	1	2	3	4	5	6	7	8
0	Z_{00}	-							
1	-	Z_{11}							
2	Z_{20}	-	Z_{22}						
3	-	Z_{31}	-	Z_{33}					
4	Z_{40}	-	Z_{42}	-	Z_{44}				
5	-	Z_{51}	-	Z_{53}	-	Z_{55}			
6	Z_{60}	-	Z_{62}	-	Z_{64}	-	Z_{66}		
7	-	Z_{71}	-	Z_{73}	-	Z_{75}	-	Z_{77}	
8	Z_{80}	-	Z_{82}	-	Z_{84}	-	Z_{86}	-	Z_{88}

12.4.1 Feature Extraction Using Zernike Moments

In all of the experiments, a total of 25 Zernike moments from orders $0 - 8$ were extracted from image database. As a feature, Zernike moments are constructed using a set of complex polynomials and are defined inside the unit circle and the radial polynomial vector. The computation of Zernike moment with order p and repetition q is shown in Table 12.2 that is labeled as Z_{pq}.

12.4.2 Binary Image Retrieval

The binary images used are the MPEG-7 Core Experiment CE Shape-1 Part B dataset that was obtained from [20] and created by the Motion Picture Expert Group (MPEG) committee. It contains 1400 binary images grouped into 70 categories.

12.4.2.1 Feature Computation of MPEG-7 Images

Table 12.3 shows the selected Zernike moments values for MPEG-7 binary images. From Table 12.3, it can be observed that Zernike moment features of Device0_1 have have small difference with features of Device0_3 and thus is efficient in retrieving and included in top 10 ranking. One can notice that the difference of Z_{22} for Device0_1 and Device0_3 is 0.2888. However, for Device9_3 which is a totally different shape with Device0_1, these features have huge differences, i.e. 32.9132.

12.4.2.2 Retrieval Ranking Results of MPEG-7

The selected retrieval ranking results for MPEG-7 image dataset is shown in Table 12.4. In this example, only five different images were selected as a query image such as Device0_1, Car1, Misk1, Device9_1 and Seasnake1. In total there are 20 image retrieval ranks for a particular category, however for testing purposes in this chapter,

Table 12.3: Example of Zernike Moments up to the 8-th order of MPEG-7 binary images.

Image	Zernike Moment Features
 Device0_1	Z_{00}=1.4009 Z_{11}=0.3794 Z_{20}=3.2850 Z_{22}=20.7452 Z_{31}=1.7197 Z_{33}=55.775 Z_{40}=55.671 Z_{42}=28.003 Z_{44}=16.5855 Z_{51}=2.5426 Z_{53}=1.3643 Z_{55}=0.4024 Z_{60}=77.506 Z_{62}= 39.7724 Z_{64}=29.333 Z_{66}=10.578 Z_{71}=28.600 Z_{73}=13.660 Z_{75}=52.1237 Z_{77}=13.465 Z_{80}=25.195 Z_{82}=117.93 Z_{84}=43.954 Z_{86}=8.7170 Z_{88}=199.69
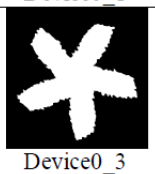 Device0_3	Z_{00}=1.1229 Z_{11}=0.6022 Z_{20}=3.4163 Z_{22}=20.4564 Z_{31}=1.7839 Z_{33}=55.628 Z_{40}=55.474 Z_{42}=28.014 Z_{44}=16.4987 Z_{51}= 2.9351 Z_{53}=1.6825 Z_{55}=0.8090 Z_{60}=77.259 Z_{62}=39.8462 Z_{64}=29.420 Z_{66}=10.289 Z_{71}=28.819 Z_{73}=13.918 Z_{75}=51.8735 Z_{77}=13.6905 Z_{80}=24.815 Z_{82}=117.86 Z_{84}=44.006 Z_{86}=8.4806 Z_{88}=199.459
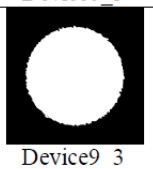 Device9_3	Z_{00}=1.1973 Z_{11}=5.2979 Z_{20}=1.6916 Z_{22}=53.6584 Z_{31}=1.9857 Z_{33}=1.1640 Z_{40}=0.9890 Z_{42}=1.6234 Z_{44}=3.5296 Z_{51}= 22.829 Z_{53}=21.797 Z_{55}=26.788 Z_{60}=161.80 Z_{62}=2.0154 Z_{64}=2.4414 Z_{66}=3.8886 Z_{71}=18.783 Z_{73}=9.0391 Z_{75}=109.369 Z_{77}=3.2586 Z_{80}=2.1795 Z_{82}=158.99 Z_{84}=63.917 Z_{86}=5.7744 Z_{88}=268.515

only the top 10 image retrieval results were displayed. From Table 12.4, it can be observed that Device0_1, Misk1 and Device9_1 give better results, since all the top 10 retrieved images are from similar categories with the query images. For the image under the category of Car1, it perfectly retrieved the first 9-th rank, however it fails to retrieve similar category under rank 10, i.e. in this case it retrieves an image under chopper category. The last query image is Seasnake1, where only rank 1 to rank 5, the system successfully retrieves similar image category, but at rank 6 to 8 it retrieves different category from query image. In rank 9, it retrieves the similar category again but then in rank 10, it again retrieves different image category. In terms of speed, on average it takes 0.0964 seconds in retrieving the similar images for Device0_1, which could be considered quite fast for a database containing more than a thousand images.

12.4.3 Grayscale Image Retrieval

The gray level images chosen in this experiment are the COIL-20 image database. COIL-20, the Columbia University Image Library [9] contains a total of 1440 grayscale images. It consists of 20 different objects and each object was captured at 72 different poses. The object was placed on a motorized turntable against a black background where the turntable was rotated through 360 degrees to vary object pose with respect to a fixed camera. Images of the object were taken at pose intervals of 5 degrees.

Table 12.4: Retrieval ranking results of MPEG-7 binary images.

Query Image	Retrieval Ranking Results									
	Rank 1	Rank 2	Rank 3	Rank 4	Rank 5	Rank 6	Rank 7	Rank 8	Rank 9	Rank 10
 Device0_1	 Device0_1	 Device0_3	 Device0_19	 Device0_4	 Device0_18	 Device0_15	 Device0_8	 Device0_20	 Device0_2	 Device0_7
Speed	0.0546 seconds	0.0773 seconds	0.0879 seconds	0.0905 seconds	0.0913 seconds	0.1007 seconds	0.1072 seconds	0.1143 seconds	0.1183 seconds	0.1219 seconds
 Car1	 Car1	 Car5	 Car6	 Car7	 Car4	 Car8	 Car2	 Car9	 Car3	 Chopper 18
Speed	0.0455 seconds	0.0633 seconds	0.0644 seconds	0.0650 seconds	0.0688 seconds	0.0751 seconds	0.0765 seconds	0.0760 seconds	0.0809 seconds	0.0821 seconds
 Misk1	 Misk1	 Misk5	 Misk20	 Misk3	 Misk16	 Misk10	 Misk2	 Misk11	 Misk14	 Misk19
Speed	0.0450 seconds	0.0619 seconds	0.2970 seconds	0.0690 seconds	0.1145 seconds	0.0807 seconds	0.0813 seconds	0.0877 seconds	0.0857 seconds	0.0893 seconds
 Device9_1	 Device9_1	 Device9_3	 Device9_4	 Device9_20	 Device9_12	 Device9_8	Device9_13	Device9_9	Device9_6	Device9_5
Speed	0.0578 seconds	0.0898 seconds	0.1029 seconds	0.0975 seconds	0.1020 seconds	0.1076 seconds	0.1150 seconds	0.1164 seconds	0.1244 seconds	0.1305 seconds
Sea Snake1	Sea Snake1	Sea Snake8	Sea Snake20	Sea Snake14	Sea Snake15	Device6_2	Device6_19	Device6_14	Sea Snake5	Bird8
Speed	0.0804 seconds	0.2896 seconds	0.0657 seconds	0.1104 seconds	0.0874 seconds	0.1453 seconds	0.1054 seconds	0.1011 seconds	0.0906 seconds	0.0992 seconds

12.4.3.1 Features Computation of COIL-20 Images

Table 12.5 shows all of the 25 Zernike moment values extracted from COIL-20 image database. For simplicity, only one of the 20 categories has been selected as the query image. From this table, it can be observed that in rank 1, it retrieves similar image as in the query because of the same features' values. In rank 4, the rotated image retrieved in top 5 of the ranking has shown and confirmed that Zernike moments are rotation invariant.

12.4.3.2 Retrieval Ranking Results of COIL-20

Table 12.6 shows the retrieval ranking results for gray scale images by using COIL-20. Five different images have been chosen as a query image and only the top 10 of the retrieved images were shown. From the results shown in Table 12.6, it can be observed that all the top 10 ranks were able to retrieve similar image categories as in the query image except for the third query where in ranking number 8, it has retrieved an object from different category. Further observation shows that Zernike moments are able to retrieve a rotated image under similar category, i.e. rank 4 in the first image query. These results show that Zernike moments' implementation for grayscale images are also efficient in retrieving similar look image as in the case of the binary images in earlier experiments.

It should be noted that the efficiency obtained under gray scale images is better than in the case of the binary images due to the number of images per image category being used. For gray scale images, in one category there are 72 images with different poses, thus the retrieval results for grayscale images are much better when compared to binary images.

12.5 Conclusion

The idea of implementing Zernike moments as feature extractor in image retrieval is that Zernike moments properties were robust to image rotation. Because of Zernike moments are defined over the unit disk, they are naturally unaffected by rotation. It is proven through the conducted experiments that Zernike moments are rotation invariant and fast computed. The image retrieval by using Zernike moments features show that they can retrieve similar looking images for both binary and grayscale images. The proposed future work is aimed to achieve other properties such as translation, scaling, occlusion and affine invariance.

References

[1] D. Agrawal, A.S. Jalal, and R. Tripathi. Trademark image retrieval by integrating shape with texture feature. In *International Conference on Information Systems and Computer Networks (ISCON)*, pages 30–33, March 2013.

[2] Sh. Akbarpour. A review on content based image retrieval in medical diagnosis. *International Journal on "Technical and Physical Problems of Engineering"*, 5(2):148–153, 2013.

Table 12.5: Example of Zernike Moments up to the 8-th order for COIL-20 gray scale images.

Types of Images		Image	Zernike Moment Features
Query Image		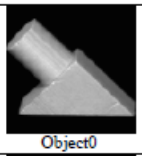 Object0	Z_{pq} = 1.0e+004 * Z_{00}= 0.3792 Z_{11}= 0.5333 Z_{20}= 0.4988 Z_{22}=0.3796 Z_{31}=0.9181 Z_{33}= 0.9845 Z_{40}= 0.7916 Z_{42}= 0.2230 Z_{44}=0.6001 Z_{51}=0.6723 Z_{53}= 0.4939 Z_{55}= 0.1219 Z_{60}= 1.4533 Z_{62}=0.9327 Z_{64}=0.5911 Z_{66}= 0.2997 Z_{71}= 1.0231 Z_{73}= 0.7392 Z_{75}=1.8035 Z_{77}=0.7950 Z_{80}= 0.9038 Z_{82}= 1.7060 Z_{84}= 0.0173 Z_{86}=1.5061 Z_{88}=4.5636
Retrieval Ranking Results of Images	Rank 1	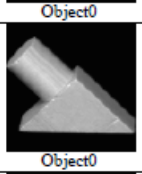 Object0	Z_{pq} = 1.0e+004 * Z_{00}=0.3792 Z_{11}=0.5333 Z_{20}=0.4988 Z_{22}=0.3796 Z_{31}=0.9181 Z_{33}=0.9845 Z_{40}=0.7916 Z_{42}=0.2230 Z_{44}=0.6001 Z_{51}=0.6723 Z_{53}=0.4939 Z_{55}=0.1219 Z_{60}=1.4533 Z_{62}=0.9327 Z_{64}=0.5911 Z_{66}=0.2997 Z_{71}=1.0231 Z_{73}=0.7392 Z_{75}=1.8035 Z_{77}=0.7950 Z_{80}=0.9038 Z_{82}=1.7060 Z_{84}=0.0173 Z_{86}=1.5061 Z_{88}=4.5636
	Rank 2	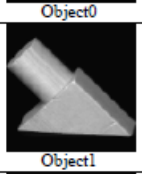 Object1	Z_{pq} = 1.0e+004 * Z_{00}=0.3360 Z_{11}=0.4928 Z_{20}= 0.4474 Z_{22}=0.3352 Z_{31}=0.8875 Z_{33}=0.8664 Z_{40}=0.7488 Z_{42}=0.1978 Z_{44}=0.5256 Z_{51}=0.5980 Z_{53}=0.4572 Z_{55}=0.1100 Z_{60}=1.4762 Z_{62}=0.9234 Z_{64}=0.6135 Z_{66}=0.2878 Z_{71}=0.9983 Z_{73}=0.7141 Z_{75}=1.7389 Z_{77}=0.7169 Z_{80}=0.8238 Z_{82}=1.5807 Z_{84}=0.1242 Z_{86}=1.4459 Z_{88}=4.6179
	Rank 3	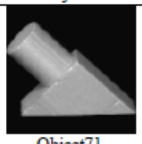 Object71	Z_{pq} = 1.0e+004 * Z_{00}=0.2866 Z_{11}=0.4056 Z_{20}=0.4321 Z_{22}=0.3338 Z_{31}=0.9097 Z_{33}=0.9745 Z_{40}=0.7289 Z_{42}=0.2214 Z_{44}=0.5879 Z_{51}=0.7300 Z_{53}=0.5389 Z_{55}=0.0492 Z_{60}=1.4462 Z_{62}=0.7307 Z_{64}=0.4276 Z_{66}=0.2184 Z_{71}=0.8471 Z_{73}=0.6270 Z_{75}=1.5890 Z_{77}=0.7728 Z_{80}=0.8835 Z_{82}=1.6378 Z_{84}=0.1664 Z_{86}=1.3236 Z_{88}=4.4054
	Rank 4	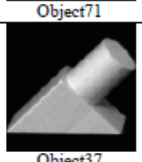 Object37	Z_{pq} = 1.0e+004 * Z_{00}=0.4219 Z_{11}=0.4870 Z_{20}=0.5461 Z_{22}=0.4121 Z_{31}=0.9283 Z_{33}=0.9947 Z_{40}=0.6807 Z_{42}=0.3165 Z_{44}=0.5535 Z_{51}=0.7332 Z_{53}=0.5409 Z_{55}=0.2017 Z_{60}=1.2958 Z_{62}=1.0262 Z_{64}=0.6121 Z_{66}=0.5130 Z_{71}=1.1812 Z_{73}=0.8257 Z_{75}=1.7899 Z_{77}=0.7039 Z_{80}=0.7756 Z_{82}=1.6178 Z_{84}=0.0774 Z_{86}=1.4871 Z_{88}=4.6071
	Rank 5	 Object36	Z_{pq} = 1.0e+004 * Z_{00}=0.4438 Z_{11}=0.5016 Z_{20}=0.5283 Z_{22}=0.4113 Z_{31}=0.9196 Z_{33}=0.9334 Z_{40}=0.6603 Z_{42}=0.2872 Z_{44}=0.5162 Z_{51}=0.6387 Z_{53}=0.4761 Z_{55}=0.2317 Z_{60}=1.3161 Z_{62}=1.0881 Z_{64}=0.6971 Z_{66}=0.5450 Z_{71}=1.2074 Z_{73}=0.8145 Z_{75}=1.8078 Z_{77}=0.6808 Z_{80}=0.6719 Z_{82}=1.5790 Z_{84}=0.0792 Z_{86}=1.4886 Z_{88}=4.6598

Table 12.6: Retrieval ranking results of gray scale images (COIL-20).

Query Image	Retrieval Ranking Results									
	Rank 1	Rank 2	Rank 3	Rank 4	Rank 5	Rank 6	Rank 7	Rank 8	Rank 9	Rank 10
 Object0	 Object0	 Object1	 Object71	 Object37	 Object36	 Object35	 Object2	 Object38	 Object3	 Object70
 Duck0	 Duck0	 Duck1	 Duck71	 Duck70	 Duck2	 Duck69	 Duck38	 Duck37	 Duck3	 Duck36
 Object7_0	 Object7_0	 Object7_71	 Object7_1	 Object7_70	 Object7_16	 Object7_2	 Object7_17	 Object11_14	 Object7_15	 Object7_18
 Object18_0	 Object18_0	 Object18_1	 Object18_71	 Object18_2	 Object18_70	 Object18_69	Object18_3	Object18_68	Object18_4	Object18_5
Object10_0	Object10_0	Object10_1	Object10_71	Object10_70	Object10_69	Object10_2	Object10_3	Object10_68	Object10_67	Object10_4

[3] C.B. Akgül, D.L. Rubin, S.Napel, C.F. Beaulieu, H. Greenspan, and B. Acar. Content-based image retrieval in radiology: current status and future directions. *Journal of Digital Imaging*, 24(2):208–22, 2011.

[4] J. Altmann and H.J.P. Reitbock. A fast correlation method for scale-and translation-invariant pattern recognition. *IEEE Transactions on Pattern Analysis and Machine Intelligence*, PAMI-6(1):46–57, 1984.

[5] F.M. Anuar, R. Setchi, and Y.K. Lai. Trademark image retrieval using an integrated shape descriptor. *Expert Systems with Applications*, 40(1):105–121, 2013.

[6] S.A. Bakar, M.S. Hitam, and W.N.J.H. Wan Yussof. Content-based image retrieval using sift for binary and greyscale images. In *Signal and Image Processing Applications (ICSIPA), 2013 IEEE International Conference on*, pages 83–88, October 2013.

[7] S.A. Bakar, M.S. Hitam, and W.N.J.H. Wan Yussof. Single object shape based image retrieval using Zernike moments. *Journal of Data Processing*, 3(1):13–20, 2013.

[8] R. Bracewell. *The Fourier Transform and its Applications*. McGraw-Hill, New York, 1965.

[9] COIL-20. Columbia university image library. [Online] - Available: http://www.cs.columbia.edu/CAVE/software/softlib/coil-20.php.

[10] S.A. Dudani, K.J. Breeding, and R.B. Mcghee. Aircraft identification by moment invariants. *IEEE Transactions on Computers*, C-26(1):39–46, 1977.

[11] A. Goyal and E. Walia. Variants of dense descriptors and Zernike moments

as features for accurate shape-based image retrieval. *Signal, Image and Video Processing*, 2012.

[12] M.K. Hu. Visual pattern recognition by moment invariants. *IRE Transactions on Information Theory*, 8(2):179–187, 1962.

[13] Q. Iqbal and J.K. Aggarwal. Cires: a system for content-based retrieval in digital image libraries. In *International Conference on Control, Automation, Robotics and Vision (ICARCV)*, volume 1, pages 205–210, December 2002.

[14] H. Jégou, M. Douze, and C. Schmid. Improving bag-of-features for large scale image search. *International Journal of Computer Vision*, 87(3):316–336, 2010.

[15] B. Jyothi, Y.M. Latha, P.G.K. Mohan, and V.S.K. Reddy. Medical image retrieval using moments. *International Journal of Application or Innovation in Engineering & Management*, 2(1):195–200, 2013.

[16] A. Khotanzad and Y.H. Hong. Invariant image recognition by Zernike moments. *IEEE Transactions on Pattern Analysis and Machine Intelligence*, 12(5):489–497, 1990.

[17] S.X. Liao and M. Pawlak. On the accuracy of Zernike moments for image analysis. *IEEE Transactions on Pattern Analysis and Machine Intelligence*, 20(12):1358–1364, 1998.

[18] B.S. Manjunath and W.Y. Ma. Texture features for browsing and retrieval of image data. *IEEE Transactions on Pattern Analysis and Machine Intelligence*, 18(8):837–842, 1996.

[19] M. Mercimek, K. Gulez, and T.V. Mumcu. Real object recognition using moment invariants. *Sadhana*, 30(6):765–775, 2005.

[20] MPEG. The moving picture expert group. [Online] Available: http://www.imageprocessingplace.com/root_files_V3/image_databases.htm.

[21] R. Mukundan, S.H. Ong, and P.A. Lee. Image analysis by Tchebichef moments. *IEEE Transactions on Image Processing*, 10(9):1357–1364, 2001.

[22] R. Mukundan and K.R. Ramakrishnan. *Moment Functions in Image Analysis: Theory and Appplications*. World Scientific, Singapore, 1998.

[23] R.J. Prokop and A.P. Reeves. A survey of moment-based techniques for unoccluded object representation and recognition. *CVGIP: Graphical Models and Image Processing*, 54(5):438–460, 1992.

[24] J. Sivic and A. Zisserman. Video google: a text retrieval approach to object matching in videos. In *IEEE International Conference on Computer Vision (ICCV)*, volume 2, pages 1470–1477, 2003.

[25] A.W.M. Smeulders, M. Worring, S. Santini, A. Gupta, and R. Jain. Content-based image retrieval at the end of the early years. *IEEE Transactions on Pattern Analysis and Machine Intelligence*, 22(12):1349–1380, 2000.

[26] M.R. Teague. Image analysis via the general theory of moments. *J. Opt. Soc. Am.*, 70(8):920–930, 1980.

[27] C.H. Teh and R.T. Chin. On image analysis by the methods of moments. *IEEE Transactions on Pattern Analysis and Machine Intelligence*, 10(4):496–513, 1988.

[28] A. Varghese, K. Balakrishnan, R.R. Varghese, and J.S. Paul. Content based image retrieval of t2 weighted brain mr images similar to t1 weighted images. In *Pattern Recognition and Machine Intelligence*, volume 8251 of *LNCS*, pages 474–481. Springer-Verlag Berlin Heidelberg, 2013.

[29] P.T. Yap, R. Paramesran, and S.H. Ong. Image analysis by Krawtchouk moments. *IEEE Transactions on Image Processing*, 12(11):1367–1377, 2003.

[30] D. Zhang, Y.L., and J. Hou. Digital image retrieval using intermediate semantic features and multistep search. In *Digital Image Computing: Techniques and Applications (DICTA)*, pages 513–518, December 2008.